Journal of Mining and Metallurgy 44 B (2008) 115 - 124

Journal of
Mining and
Metallurgy

VOLTAMMETRIC INVESTIGATIONS OF ANODIC DISSOLUTION OF NATURAL MINERAL CHALCOPYRITE

M. Vuković, Z. D. Stanković, M. Rajčić-Vujasinović* and V. Cvetkovski**

*University of Belgrade, Technical Faculty Bor, 19210 Bor, Serbia and Montenegro,
**Institute for Mining and Metallurgy Bor, 19210 Bor

(Received 01 February 2008; accepted 26 February 2008)

Abstract

Anodic oxidation of the natural mineral chalcopyrite from the Bor ore deposit has been studied by cyclic voltammetry in pure sulfuric acid solutions. At the obtained voltammograms, the appearance of peaks at certain potential regions was identified and found to be much less pronounced than those previously reported in the literature. The voltammetric kinetic analysis confirmed that two-electron exchange electrochemical reactions occur. The explanation for this somewhat different electrochemical behavior of natural chalcopyrite compared to the concentrates widely used in studies of this mineral will also be given.

Keywords: Natural chalcopyrite, anodic dissolution, voltammetry, prewave.

1. Introduction

The electrochemical behavior of chalcopyrite has been studied by many authors in order to obtain information about the kinetics and mechanism of chalcopyrite dissolution [1-15].

Different electrochemical techniques were applied in these studies, such as: linear sweep voltammetry, cyclic voltammetry, potentiodynamic method, chronopotentiometry, chronoamperometry, galvanostatic method and, recently, the rotating ring-disc method [13]. An excellent review of various mechanisms reported in the literature can be found in the paper by J.B. Hiskey [9].

* *Corresponding author: mvukovic@tf.bor.ac.yu*

DOI:10.2298/JMMB0801115V

In spite of different reported mechanisms, there is agreement that electrochemical behavior of chalcopyrite in acidic solutions reveals two distinct regions: (i) Low potential range (0.2-0.7 V vs. SCE) where the passivation reaction occurs, causing formation of a progressively thickening surface film, and, (ii) high potential range (1.0-1.2 vs. SHE) where the anodic oxidation of chalcopyrite ends up [9].

Recently, Rodriguez et al.[12] showed that the oxidation state of the dissolved iron (Fe^{3+}) was fundamental to chalcopyrite bioleaching because Fe^{3+} controlled the relative rate of the oxidation reactions. In addition, the attack of chalcopyrite was controlled by elemental sulphur and intermediate, nonstoichiometric, copper sulphides forming on the chalcopyrite surface, which are less reactive than the original sulphide. Intermediate sulphides caused an important barrier effect at low temperature (35 ^{o}C). At higher temperature (68 ^{o}C) these intermediate sulphides do not constitute a diffusion barrier due to their dissolution.

A passive region is critical to develop and understand the intrinsic electrochemisty of chalcopyrite. According to G.W. Warren et al.[2] and T. Biegler et al.[5], the initial oxidation of chalcopyrite can be characterized by the preferential release of iron from the lattice and by the formation of an intermediate defect structure [2,5]. A.J. Parker et al.[3] suggested that the initial oxidation of chalcopyrite produces a metal-deficient polysulfide similar to that of CuS2. This passive layer reaches an equilibrium thickness and, then, decomposes.

Biegler et al.[1] studied the electrochemical behavior of chalcopyrite at low potentials and noticed the anodic prewaves

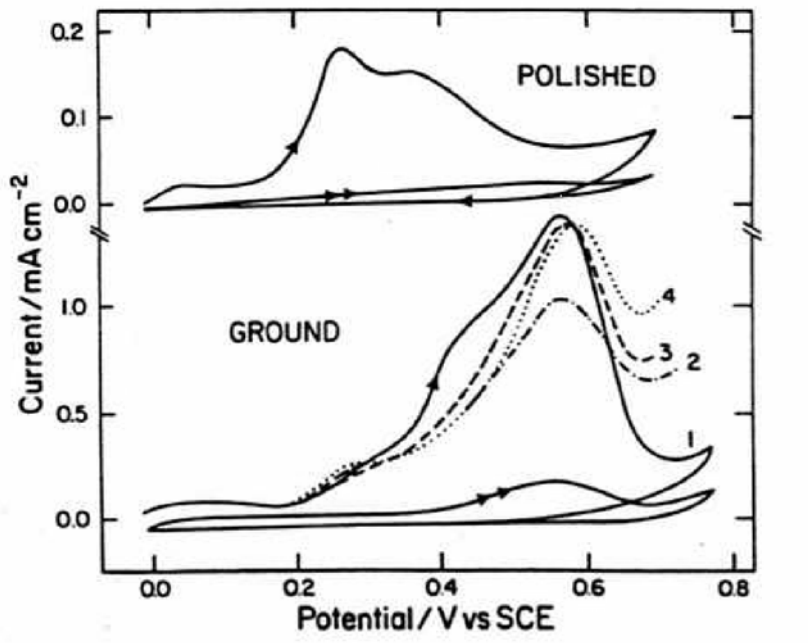

Fig. 1. Voltammograms for $CuFeS_2$ oxidation at 20 mV/s and 50 rev/s. (a) Polished electrode in 1 M HCl, (b) Ground electrode in 1) 1 M HCl, 2) 1 M HNO_3, 3) 1 M H_2SO_4 and 1 M $HClO_4$

for chalcopyrite dissolution in various acid electrolytes (Fig. 1). The voltammogram for a polished chalcopyrite electrode clearly reveals two prewave peaks at about 0.28 and 0.38 V (vs. SCE). The ground electrode shows two shoulders, which correspond to the prewave peaks seen on the polished electrode. The prewave process represents the initial oxidation of chalcopyrite and reflects the formation of passive surface product layers. It was calculated that the ratio of cathodic charge to anodic charge is 1.3. Bauer et al.[9] studied the initial-stage leaching of chalcopyrite in sulfuric acid and oxygen and noticed that the Fe/Cu ratio changes from 6.6 (30 s) to 3.5 (10 min).

It seems that differences in the behavior of chalcopyrite likely result from inherent differences in the semi-conducting characteristics of the various sources of chalcopyrite used in each of these studies. The conductivity (i.e., resistivity) is probably the most important measure of the semiconducting nature of sulfides. In the case of natural samples of chalcopyrite, n-type semiconducting is much more pronounced than p-type, i.e., the free charge carrier must be metal in excess of the stoichiometric amount occurring primarily as metal interstitials [16,17]. In addition, the presence of other minerals in the chalcopyrite makes comparison of different data more complicated. Other phases present could, for instance, create a complex galvanic couple. The crystal structure, grain size, porosity, and history of the mineral will affect reaction rate as well [18].

In this paper, chalcopyrite anodic dissolution is studied, using cyclic voltammetry in the low potential region, i.e., within the passive area. The purpose of this research is to examine the electrochemical behavior of one source of chalcopyrite (from the Bor-Mines, Eastern Serbia) immersed in sulfuric acid solution without the presence of a chemical oxidant. The obtained results are correlated with those that have already been reported for chalcopyrite from other sources.

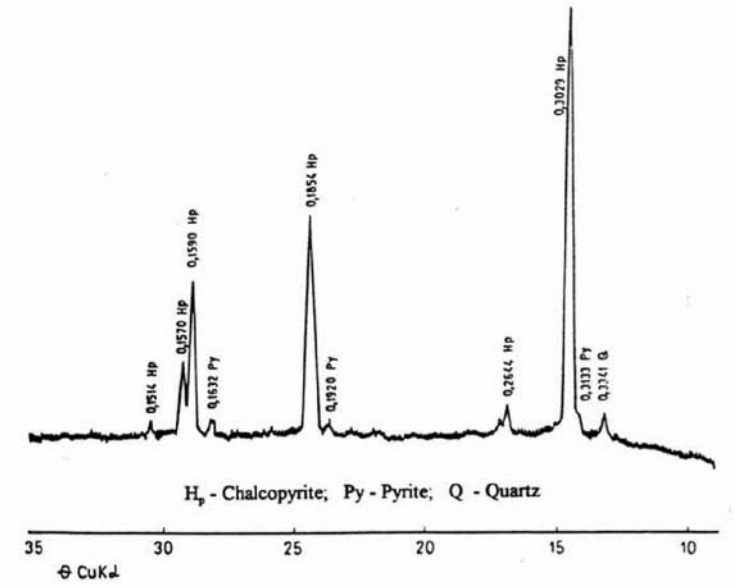

Fig. 2. X-ray analysis of natural chalcopyrite form the Bor ore deposit

2. Experimental

Fig. 2 illustrates the working electrode made of natural chalcopyrite mineral from the Bor ore deposit. X-ray analysis showed that the natural chalcopyrite contained some amounts of pyrite and quartz (Fig. 3). The purity of the natural mineral was very high. The sample was dipped in the "Simplex"

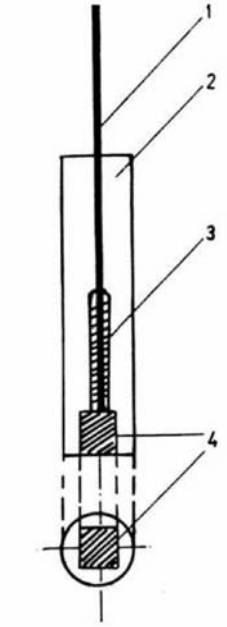

Fig. 3. Illustration of the electrode used: 1) Copper wire, 2) electrode body; 3) mercury, and 4) chalcopyrite. A = 0.20 cm^2

mass for cool samples dipping. Electrical contact was provided by means of mercury and copper wire, as described by Sato [19]. The counter electrode was made of platinum sheet of 20 x 5 x 0.05 mm with a total surface area of 1 cm2.

The reference electrode was a saturated calomel electrode (SCE) and all potentials are quoted with respect to the SCE. Measurements were carried out at 25 ^{o}C in nitrogen-purged solutions prepared from doubly distilled water and reagent-grade chemicals. Programmed voltammetry was carried out with conventional instrumentation (potentiostat-galvanostat, Amel-model 551).

Before immersion in the electrochemical cell (Amel-model 494 GC + 494 TJ), the working electrode was freshly prepared prior to each experiment by:

- grinding on the finest paper used for the metallographic sample preparation;
- wet polishing on alumina (waterproof cloth soaked in alumina suspension of 0.5 μm in distilled water);
- rinsing in water, distilled water and alcohol and drying in air, and, finally;
- rinsing with a working solution.

This is a fairly standard preparation procedure before an electrochemical experiment, although other courses of preparation were also tested (as will be shown later).

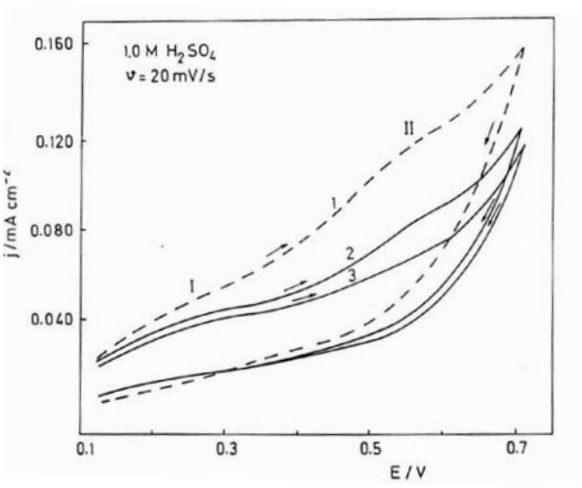

Fig. 4. Voltammograms for natural chalcopyrite; sweep rate 20 mV/s; preparation courses: 1) ground electrode, 2) polished electrode, 3) polished and rinsed electrode

3. Results and Discussion

Fig. 4 shows the voltammograms obtained for chalcopyrite immediately immersed in the 1.0 M H_2SO_4 solution after preparation course. All the voltammograms were obtained at the scan rate of 20 mVs^{-1}, starting from the open-circuit potentials (130 mV vs. SCE). Different electrode preparation procedures were applied such as: Grounding, polishing, and polishing followed by the ethanol and working solution rinsing (curves 1, 2, and 3, respectively). Thus, in all cases, the prewave region appears and it can be distinguished as follows: First, there is a so-called prewave I, at potential of about 280 to 300 mV vs. SCE, and, a second one, so-called main wave II (towards more positive potentials) at potential of about 560 mV vs. SCE. These potentials are in agreement with those reported by Biegler et al. [1] (Fig. 1). Yet, some differences are worth analyzing. For instance, no two different peaks before the main prewave peak are noticed in this study. This was not the case in the previously cited work [1] (peaks at potentials of 0.28 and 0.38 mV vs. SCE). Another important feature of voltammograms, presented in Fig. 4, is the presence of slightly pronounced prewaves.

The shape, position, charge quantity, and area of prewaves depend on a chosen preparation course – especially in the case of main prewave. At the lowest peak, current was obtained when the polishing was followed by rinsing with a doubly distilled water and sulfuric acid solution, and all further experiments were performed with electrode prepared in this way.

The influence of exposure of the fresh chalcopyrite surface to air is shown in Fig. 5.

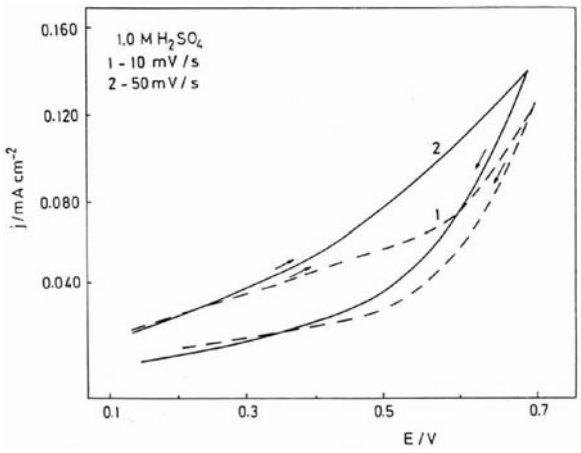

Fig. 5. Voltammograms for chalcopyrite immersed in 1.M H_2SO_4 after 30 min exposure to air; 1) v=10 mV/s and 2) v=50 mV/s

The voltammograms were obtained after 30 minutes of the chalcopyrite exposure to air. No significant effect of oxygen was noticed since the maximum peak current was almost the same as that reported in Fig. 4 – around 0.120 mA cm^{-2}. If preoxidation had occurred, the current should decrease, but this was not observed in this experiment. A similar effect had been noticed earlier [1].

However, under these conditions – exposure to air, 30 min – the prewaves on voltammograms disappear even at a scan rate of 50 mVs^{-1}, at which these prewaves were strongly expressed (Fig. 6). A possible explanation of this difference is the presence of impurities in the natural chalcopyrite (See Fig. 3.). W.K. Choi [20] obtained, for example, under the similar electrochemical conditions (no rotating disc electrode), well-pronounced peaks in both the sterile and innoculated nutritient solution – pH=2.3, adjusted with H_2SO_4 – containing *Thiobacillus ferrooxidans* bacteria. A high-

grade chalcopyrite concentrate (Fig. 7) was used here for preparation of the electrode coated with 10%-carbon paste [20]. However, Arce and Gonzalez [21], using carbon paste electrodes containing mineral with nonconducting binder, showed that the chalcopyrite oxidation process did not produce covellite as claimed by others. Chalcopyrite oxidation has been found to produce a nonstoichiometric sulphide, $Cu_{n-1}Fe_{n-1}S_{2n}$.

Earlier, G.W. Warren [2] showed that the chalcopyrite from various localities behaves quite differently under identical conditions of anodic dissolution (a potentiodynamic method was used). This means that

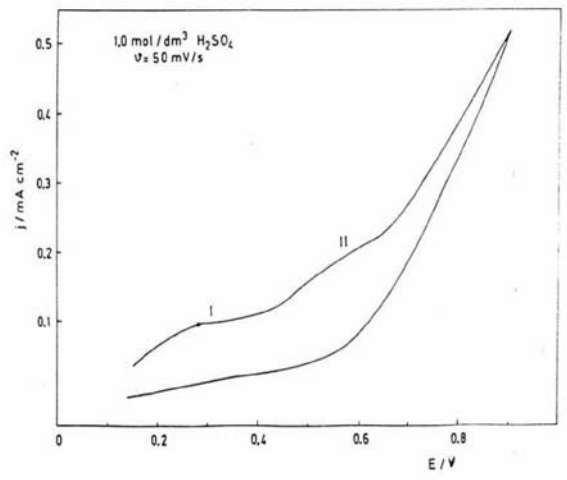

Fig. 6. Voltammogram for chalcopyrite in 1 M H_2SO_4; v=50 mV/s

completely different kinetic mechanisms can be observed in identical leaching systems, i.e., mixed potential systems using minerals from various sources. It was assumed that this behavior results from the variable nature of the surface layer and maybe also from minute differences in the electronic properties of the mineral. For instance, the presence of cubanite was responsible for an

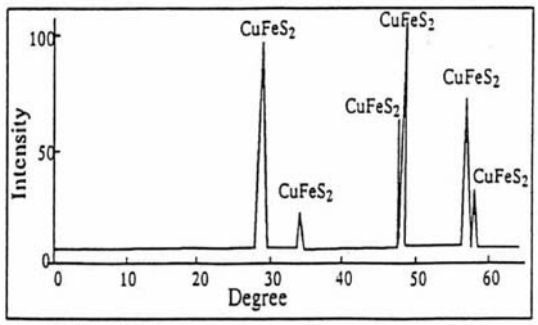

Fig. 7. X-ray diffraction pattern of chalcopyrite concentrate [20s]

increased current for the two minerals investigated [18].

Prewaves I and II (shown in Fig. 6) are connected with the dissolution of chalcopyrite during its bioleaching. There are several candidate reactions that can describe the anodic chalcopyrite dissolution in a passive region. Yet, on the basis of the experimental results presented here, the following electrochemical reactions can be attributed to the peaks observed in Fig. 6:

Peak I: (Eo = 0.53 V vs. SHE)

$$Cu_2S \rightarrow CuS + Cu^{2+} + 2e \quad (1)$$

Peak II: (Eo = 0.86 V vs. SHE)

$$CuS + 2H_2O \rightarrow Cu(OH)_2 + S^o + H^+ + 2e \quad (2)$$

As can be seen from the stoichiometry of reaction (2), it includes elemental sulfur as a reaction product of chalcopyrite oxidation in acidic solutions. However, the formation of massive layers of elemental sulfur can mask the very subtle and sometimes elusive electrochemical effects. Experimental electrochemical data presented here

demonstrate that the formation of surface film during anodic reactions can greatly affect dissolution behavior. One can expect the formation of a thin metal-deficient surface layer in the low "passive" region.

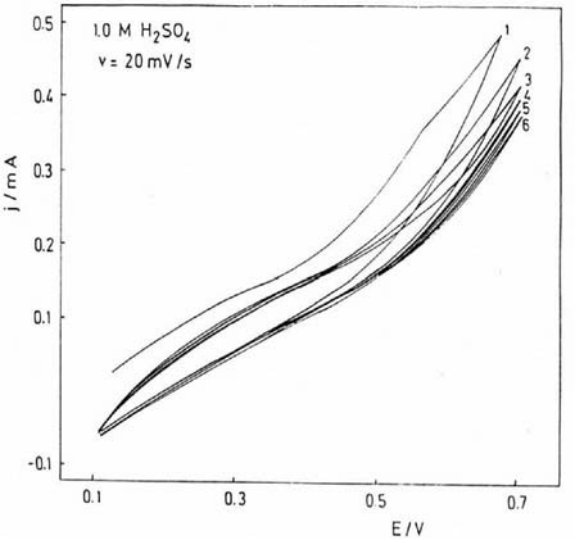

Fig. 8. Repeated cyclic voltammograms for chalcopyrite in 1 M H_2SO_4; v=20 mV/s

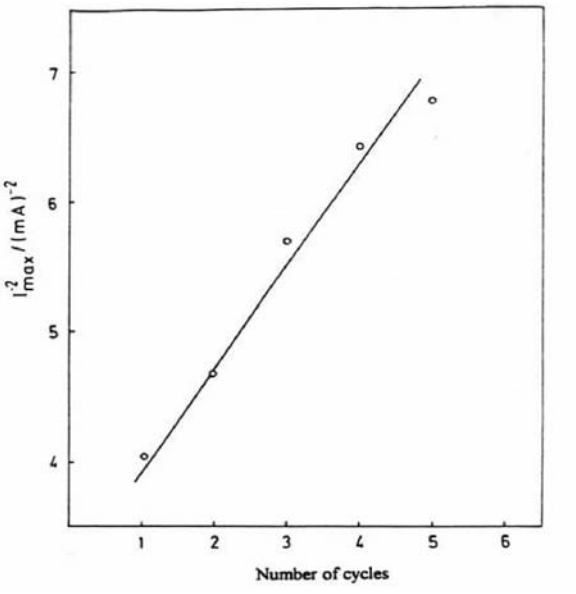

Fig. 9. A reciprocal peak current value as a function of number of cycles (Data from Fig. 8)

J.B. Hiskey [9] reported that this layer is a mixture of CuS and S^o, and that it reaches a steady-state thickness of about 3 nm.

The repeated cyclic voltammograms in sulfuric acid solution are shown in Fig. 8.

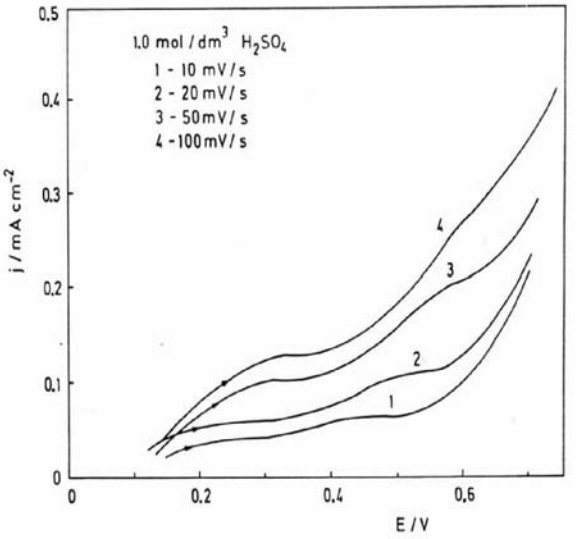

Fig. 10. Anodic polarization curve for chalcopyrite in 1 M H_2SO_4 at different scan rates:1) 10, 2) 20, 3) 50, and 4) 100 mV/s

When the cyclic voltammogram was repeated, the height of a maximum peak current continuously decreased (Fig. 9). The decrease in the peak currents corresponds to the disappearance of active species from the surface of chalcopyrite, i.e., accumulation of a prewave product layer. In this manner, the active electrode surface decreases. A similar effect was noticed by other investigators [1,22,23]. Fig. 8 also shows that the prewave has essentially already disappeared after the second cycle.

The anodic polarization curve for chalcopyrite obtained at various scan rates (scan range of 10 to 100 mV/s) are shown in Fig. 10. Polarization was performed in the anodic direction, starting from the open-

circuit potential to 0.70 V vs. SCE. At the higher scan rates, previously mentioned Peaks I and II are more pronounced. Also, a slightly noticeable shift of peaks to more positive potentials as well as an increase in peak currents was noticed.

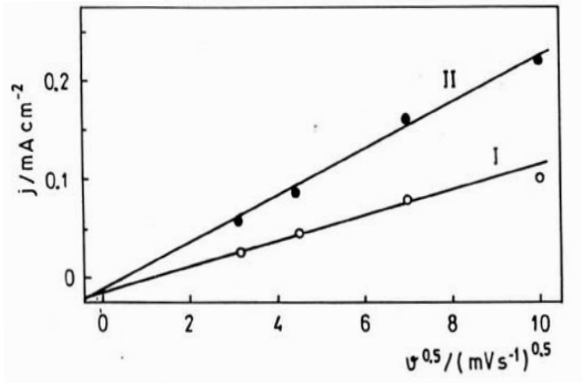

Fig. 11. Dependencies of the peak currents (I and II) on the square root of the scan rate; (Data from Fig.10)

An analysis of these data shows a linear relationship between the square root of the scan rate and the maximum peak current for both Peak I and Peak II (This is illustrated in Fig. 11.). The obtained dependence allows us to conclude that the influence of diffusion exists and cyclic voltammetry is more available for identification of a number of steps in the overall reaction where it can be useful as a qualitative method. Certainly, there is a possibility for kinetic determinations in the case where the mechanism of a certain reaction has been previously discovered. As the chalcopyrite dissolution is a typical irreversible reaction, it is possible to use the relation:

$$b = 2 \times (d E_p / d \log v) \quad (3)$$

where b is the Tafel coefficient.

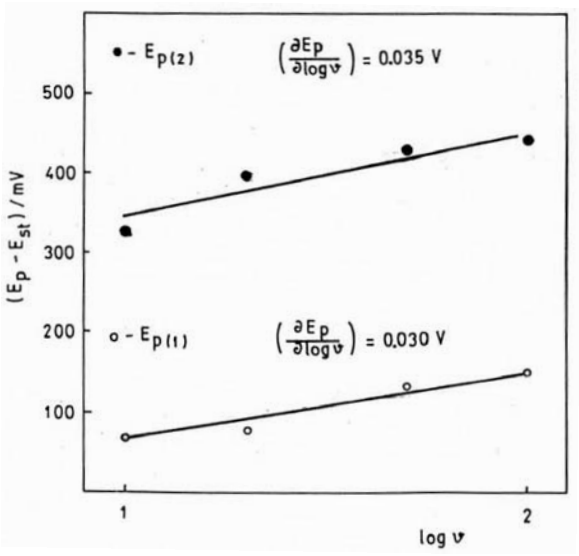

Fig. 12. Dependencies (E_p - E_s) vs. log v for chalcopyrite in 1 M H_2SO_4

In Fig. 12, potential E_p corresponding to the difference between potentials at which Peak I and Peak II appear and stationary potential E_s was presented as a function of logarithm of scan rate. The obtained values for the slope (d E_p / d log v) for Peak I and Peak II (0.030 and 0.035 V/dec, respectively) are in agreement with the theoretically expected Tafel slopes for two-electron exchange electrochemical reactions. These values have already been obtained during the galvanostatic measurements in all the studied systems with the exception of the one that contained ferric ions at higher overpotentials [6,24]. Clearly, the voltammetric results presented here confirm the chalcopyrite anodic dissolution mechanism proposed on the basis of galvanostatic measurements [24].

Thus, by using the relation (3) for the reaction occurring at potentials of about 280 mV vs. SCE, the following results:

$b = 2 \times (d E_p (1) / d \log v) = 2 \times 0.030$

$b = 0.060$ V

while for the reaction at higher potentials (up to about 700 mV vs. SCE), the appropriate expression follows:

$b = 2 \times (d E_p (2) / d \log v) = 2 \times 0.035$

$b = 0.070$ V

According to the relation:

$b = 2 \times (2.303\ RT / \alpha_a F)$

where R is the universal gas constant, T is the absolute temperature, and F is the Faraday's constant, the corresponding anodic transfer coefficients, α a, in terms of Peak I and Peak II, are determined as:

$\alpha_{a\,(1)} = 0.98 \approx 1$ and

$\alpha_{a\,(2)} = 0.84 \approx 1$

The values calculated above correspond to the two-electron exchange reactions. In other words, reactions (1) and (2), previously considered on the basis of thermodynamic expectations, may be appropriate to describe the chalcopyrite anodic dissolution in a passive region in the sulfuric acid solution.

4. Conclusion

The anodic prewave indentified on the voltammograms for freshly prepared natural chalcopyrite electrodes in sulfuric acid solutions represents a surface oxidation process which is distinct in the mechanism from the bulk oxidation of chalcopyrite observed at higher potentials. The importance of the prewave is that it allows insight into the mechanism of oxidative dissolution of chalcopyrite. The nature of the prewave reactions, determined from the kinetic information obtained by cyclic voltammetry, as well as the reaction sequence $2CuFeS_2 \rightarrow Cu_2S \rightarrow CuS$, suggests two-electron exchange electrochemical reactions. The results presented in this paper confirm the previously well-known fact that for any natural chalcopyrite sample taken from other deposits, the anodic dissolution behavior may be quite different than that expected for the same experimental conditions.

Acknowledgments

We thank Mr. Zoran Stevic for providing the software program for the voltammetric measurements used in this work.

References

1. T. Biegler and M.D. Horne, *J. Electrochem. Soc.*, 132 (1985) 1363.

2. G.W. Warren, M.E. Wadsworth and S.M. El-Raghy, *Metall. Trans. B*, 13B (1982) 571.

3. A.J. Parker, R.L. Paul and G.P. Power, *J. Electroanal. Chem.*, 118 (1981) 305.

4. R.S. McMillan, D.J. MacKinnon and J.E. Dutrizac, *J. Appl. Electrochem.*, 12 (1982) 743.

5. T. Biegler and D.A. Swift, *J. Appl. Electrochem.*, 9 (1979) 545.

6. Z.D. Stankovic, *Erzmetall*, 39 (1986) 623.

7. H.G. Linge, *Hydrometallurgy*, 2 (1976) 51.

8. X. Cheng, K.A. Smith and I. Iwasaki, in "Electrochemistry of chalcopyrite-pyrrhotite-mild steel interactions", The Paul E. Int. Symp. Extractive Metallurgy of Copper, Nickel and Cobalt Volume I: Fundamental Aspects (Ed. by R.G. Reddy and R.N. Weizenbach), The Minerals, Metals and Materials Society, 1993, p. 971.

9. J. B. Hiskey, in "Electrochemistry of chalcopyrite-pyrrhotite-mild steel interactions", The Paul E. Int. Symp. Extractive Metallurgy of Copper, Nickel and Cobalt Volume I: Fundamental Aspects (Ed. by R.G. Reddy and R.N. Weizenbach), The Minerals, Metals and Materials Society, 1993, p. 949.

10. Z.Y. Lu, M.I. Jeffrey and F. Lawson, *Hydrometallurgy*, 56 (2000) 145.

11. A.E. Elsherief, *Mineral Processing*, 15 (2002) 215.

12. Y. Rodriguez, A. Ballestera, M.L. Blazquez, F. Gonzalez and J.A. Munoz, *Hydrometallurgy*, 71 (2003) 47.

13. I. Lazaro and M.J. Nicol, *Journal of Appl. Electrochem.*, 36 (2006) 425.

14. L. Pikna, J. Cama and T. Grygar, *Chemical Papers*, 60 (2006) 293.

15. P. Acero, J. Cama and C. Ayora, *European Journal of Mineralogy*, 19 (2007) 293.

16. D.F. Pridmore and R.T. Shuey, *American Mineralogist*, 61 (1976) 248.

17. R.T. Shuey, Semiconductiong Ore Minerals, Elsevier Publ. Co., New York, 1975.

18. G.W. Warren, Dissertation, The University of Utah, 1978, p. 7.

19. M. Sato, Econ. Geol. 55 (1960) 1202.

20. W.K. Choi, Dissertation, New Mexico Institute of Mining and Technology Socorro, New Mexico, 1990, p. 66.

21. E.M. Arce and I. Gonzalez, *International Journal of Mineral Processing*, 67 (2002) 17.

22. J. Gerlach and E. Küzeci, *Hydrometallurgy*, 11 (1983) 343.

23. M. Rajcic-Vujasinovic, Dissertation, University of Belgrade, 1989.

24. M. Vukovic, Unpublished results.